Tsunami signals from the 2006 and 2007 Kuril earthquakes detected at a seafloor geomagnetic observatory

Hiroaki Toh,[1] Kenji Satake,[2] Yozo Hamano,[3] Yushiro Fujii,[4] and Tadanori Goto[5]

Received 22 July 2010; revised 22 November 2010; accepted 2 December 2010; published 24 February 2011.

[1] A seafloor geomagnetic observatory in the northwest Pacific detected clear electromagnetic (EM) variations associated with tsunami passage from two earthquakes that occurred along the Kuril Trench. Previous seismological analyses indicated that the M8.3 earthquake on 15 November 2006 was an underthrust type on the landward slope of the trench, while the M8.1 earthquake on 13 January 2007 was a normal fault type on the seaward side. The EM measurements enabled precise monitoring of the tsunami propagation direction as well as particle motion of the seawater. The estimated horizontal water velocity differs significantly for the 2006 and 2007 tsunamis, in terms of initial motion and dispersive characters, being consistent with the hydrodynamic simulation results of the tsunamis. Namely, the tsunami-induced horizontal geomagnetic components showed opposite signs for the rise and retreat waves as expected from the "electric current wall hypothesis." The dispersion effect is more remarkable in the 2007 event with a smaller source region of its tsunamigenic earthquake. The 2007 tsunamis, therefore, tend to violate the long-wave approximation. The Boussinesq approximation was required to reproduce the dispersive character of the 2007 event in our numerical simulation. In terms of tsunami forecast, an important advantage of EM sensors over conventional tsunami sensors, such as seafloor pressure gauges, is their capability of vector measurements: in addition to their ability to monitor particle motions, the first peak of the downward magnetic component always precedes the tsunami peak, suggesting a significant improvement in global tsunami warning systems if vector EM sensors are integrated into the existing systems.

Citation: Toh, H., K. Satake, Y. Hamano, Y. Fujii, and T. Goto (2011), Tsunami signals from the 2006 and 2007 Kuril earthquakes detected at a seafloor geomagnetic observatory, *J. Geophys. Res.*, *116*, B02104, doi:10.1029/2010JB007873.

1. Introduction

[2] Giant (M > 9) earthquakes occurring along the world's subduction zones produce transoceanic tsunamis and cause serious damage at the coast. For instance, the 2004 Sumatra-Andaman earthquake (M9.2) incurred more than 230,000 tsunami casualties around the Indian Ocean including Somalia [*Bernard and Robinson*, 2009; *Lay et al.*, 2005; *Titov et al.*, 2005]. This tsunami motivated the international society to construct global tsunami warning systems, which includes seismic and sea level monitoring instruments. The 27 February 2010 Chilean earthquake (M8.8) caused considerable tsunami damage to aquaculture along the Pacific coast of northeast Japan but associated no victims thanks to pertinent tsunami early warning [*Satake et al.*, 2010]. Offshore sea level measurements using bottom pressure gauges are proved useful for detection/warning of tsunamis before their arrivals at the coast [*Bernard and Robinson*, 2009]. Deep-ocean Assessment and Reporting of Tsunamis (DART) system (http://www.ndbc.noaa.gov/dart.shtml), in which data from bottom pressure gauges are first transmitted acoustically to surface buoys and then to data centers on land via satellites, has been installed in both the Pacific and Indian oceans by NOAA and other national agencies [*Bernard and Robinson*, 2009].

[3] Seawater is known to be a good conductor with mean electrical conductivity, σ_{sw}, of 3–4 S m^{-1}. It is also known since the discovery of EM induction phenomena that a conductive medium moving relative to an ambient magnetic field can generate electric currents by a physical process called 'dynamo effect'. One of the very first proponents of the theory of EM induction was even the first to make an attempt to detect the electromotive force in a moving geophysical fluid, i.e., the estuarine water of the Thames [*Faraday*, 1832]. Large-scale motions of the conducting seawater, therefore, can produce EM fields in the ocean by

[1]Data Analysis Center for Geomagnetism and Space Magnetism, Kyoto University, Kyoto, Japan.
[2]Earthquake Research Institute, University of Tokyo, Tokyo, Japan.
[3]Institute for Research on Earth Evolution, Japan Agency for Marine-Earth Science and Technology, Kanagawa, Japan.
[4]International Institute of Seismology and Earthquake Engineering, Building Research Institute, Tsukuba, Japan.
[5]Graduate School of Engineering, Kyoto University, Kyoto, Japan.

0148-0227/11/2010JB007873

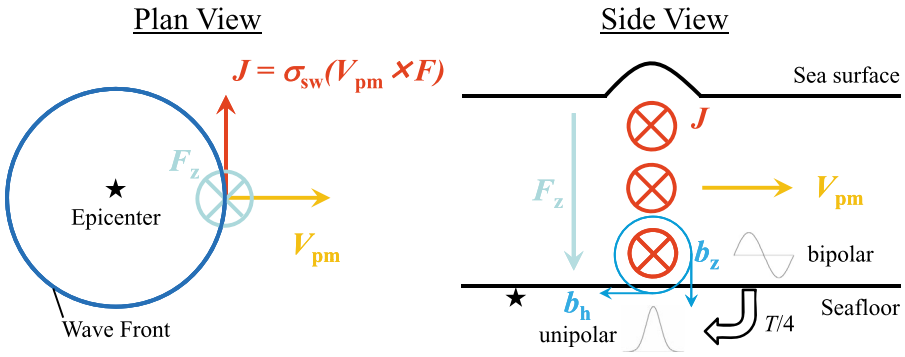

Figure 1. (left) Plan and (right) section views of the EM field in the ocean associated with tsunami propagation. As the wavefront moves radially away from the epicenter, it induces a circular curtain of electric current, $\boldsymbol{J}$, within the ocean by coupling of tsunami particle motion ($\boldsymbol{V}_{\mathbf{pm}}$) with the downward component (F_z) of the geomagnetic main field, $\boldsymbol{F}$. At the time of the tsunami passage, the seafloor horizontal geomagnetic component ($\boldsymbol{b}_{\mathbf{h}}$) perpendicular to the tsunami front always shows unipolar variations, while the downward component (b_z) of the tsunami-induced magnetic field always shows bipolar variations when observed at a fixed point on the seafloor. T is the dominant period of the tsunami in concern.

coupling with the weak but significant magnetic field of our planet. Previous studies on the oceanic dynamo theory [*Longuet-Higgins*, 1949; *Sanford*, 1971; *Chave and Luther*, 1990] revealed that the seafloor EM field is a good measure of barotropic ocean currents. On the other hand, observation of the motionally induced EM field at the seafloor has been limited to electric field measurements mostly by submarine cables [*Larsen and Sanford*, 1985; *Fujii and Chave*, 1999; *Nolasco et al.*, 2006], although seafloor electric measurements by point sensors can delineate ocean dynamics as well [*Luther et al.*, 1991; *Segawa and Toh*, 1992].

[4] Recently, long-term seafloor EM observation has been made possible even in open oceans [*Toh et al.*, 2004, 2006] with advent of low-power EM sensors as well as sustainable data recording systems developed for use at the deep seafloor. It was found that the seafloor geomagnetic observatory in the northwest Pacific succeeded in capturing tsunami-induced EM signals including not only the geoelectric but also geomagnetic field [*Toh et al.*, 2009]. This is because particle motion of seawater associated with tsunami waves is quite coherent and barotropic; the horizontal motion is the same throughout the ocean layer for a given instant and location in the long-wave approximation. The intent of this paper is to make a brief report on the tsunami-induced EM signals observed at the seafloor. In the following, first, both theoretical and observational aspects of the tsunami-induced EM signals will be described together with general hydrodynamic features of tsunamis as barotropic flows in the ocean, followed by presentation of real data. Second, the electromagnetically estimated tsunami particle motions will be further examined by comparison with hydrodynamic simulation results using both linear long-wave and Boussinesq approximation. Finally, potential of the EM sensors as tsunami detectors will be discussed and concluded.

2. Tsunami-Induced EM Signals at the Seafloor

[5] Tsunami is a gravity wave, which propagates through the ocean with a dispersive phase velocity, $c = \sqrt{\frac{g\lambda}{2\pi}\tanh\frac{2\pi d}{\lambda}}$, where g, d and λ are the Earth's gravitational acceleration, the ocean depth and the tsunami wavelength, respectively. For tsunamis from great earthquakes (M > 8), the typical wavelength λ becomes several tens to hundreds kilometers, much larger than the water depth d. If $\lambda \gg d$, the long-wave (or shallow water) approximation is, to first order, valid where the phase velocity reduces to $c = \sqrt{gd}$ without dis-

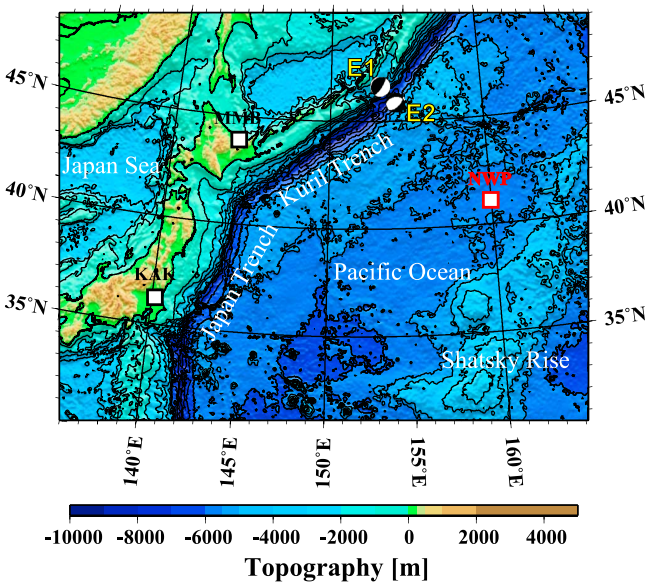

Figure 2. Epicenters of the two tsunamigenic earthquakes (E1 and E2) occurred during the seafloor EM observation at NWP from 14 July 2005 through 29 April 2007. The pair of earthquakes occurred on the landward and seaward slopes of the Kuril trench. The tsunamis by the Mw 8.3 earthquake on 15 November 2006 (E1) and the Mw 8.1 earthquake on 13 January 2007 (E2) showed opposite initial motions reflecting the nearly opposite focal mechanisms. Locations of the closest geomagnetic observatories on land (KAK and MMB) are also shown. Geomagnetic data at these observatories were used for examination of the observed EM time series at NWP as well as degree of external geomagnetic disturbance.

Table 1. Metadata of the Two Earthquakes and Site NWP

	Latitude (°N)	Longitude (°E)	Depth (km)	Distance to NWP (km)
E1	46.59	153.27	13	820.4
E2	46.24	154.52	16	727.3
NWP[a]	41.10	159.96	5.58	-

[a]The seafloor geomagnetic observatory at NWP measures the EM fields every two minutes with resolutions of 0.01 nT and 0.64 μV/m for the magnetic and electric fields, respectively.

persion. The second-order approximation is the linear Boussinesq approximation that retains dispersion effects [e.g., *Bernard and Robinson*, 2009]. Although the velocity of particle motions, $\boldsymbol{V}_{\mathbf{pm}}$, is very small (typically 1–10 mm s^{-1} in the deep ocean) [e.g., *Bryan*, 1987], they are coherent enough to create observable EM fields at the seafloor by coupling mostly with the downward component, F_z, of the geomagnetic main field, $\boldsymbol{F}$. Resultant current wall, $\boldsymbol{J}$, in the ocean is so closely tied with the tsunami wavefront that it can generate unipolar temporal variations of the horizontal geomagnetic components at the time of the tsunami passage while those of the downward component are bipolar when the tsunami-induced EM field is observed at a fixed point on the seafloor (Figure 1). Namely, the tsunami-associated downward magnetic component must change signs before and after tsunami passage for a stationary observer at the seafloor. Because horizontal EM components at the seafloor are very sensitive to the conductivity-weighted vertical average of ocean flows [e.g., *Sanford*, 1971], the motional induction signals are a good measure of barotropic flows in the ocean such as tsunamis.

[6] Particle motion of the seawater can be estimated from motionally induced EM components. According to *Sanford*'s [1971] theory of the EM induction by the oceanic dynamo effect, the observed EM field consists of local and regional terms (see equations (26) and (28)–(30) of *Sanford* [1971]) in the sense that the local term reflects contribution of coupling between the in situ horizontal velocity over the seafloor site in the measuring frame (V_x and V_y) and the downward component (F_z) of the ambient geomagnetic field, while the regional term arises from the electric currents in the Earth and the ocean integrated over a regional scale. However, simultaneous measurements of the horizontal EM components at the seafloor can be combined to eliminate the regional terms and give the local velocity components in terms of the observed EM components as follows:

$$V_x = \frac{1}{F_z}\left((1-k)E_y + \frac{2b_x}{\mu\sigma_{sw}d}\right), \tag{1}$$

$$V_y = \frac{1}{F_z}\left(-(1-k)E_x + \frac{2b_y}{\mu\sigma_{sw}d}\right), \tag{2}$$

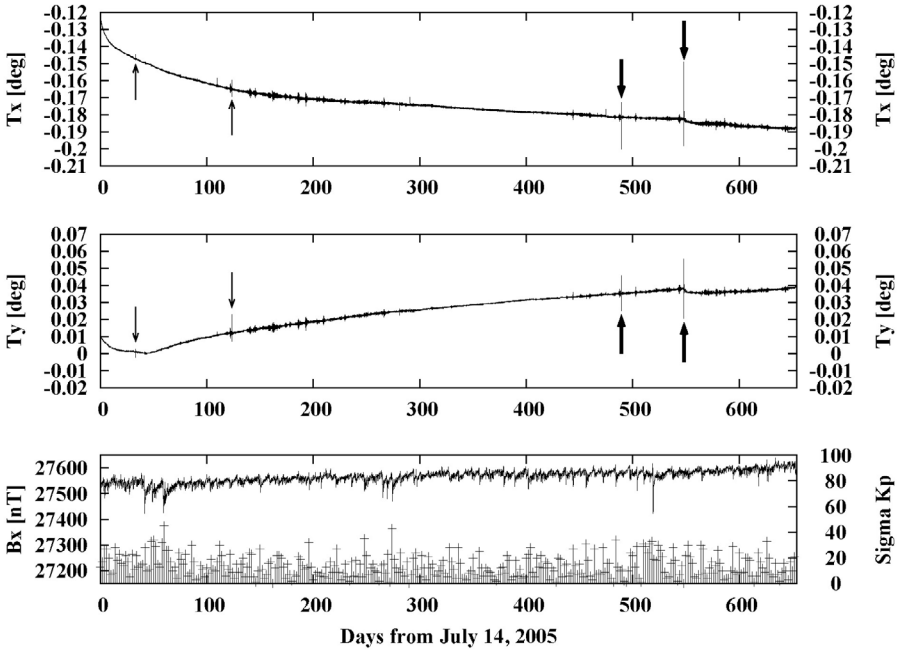

Figure 3. (top and middle) Observed horizontal tilt components and (bottom) simultaneous northward geomagnetic variations for 654 days at NWP. Thick vertical arrows indicate the tilt variations at the arrival of seismic waves of the 2006 and 2007 earthquakes. The thin arrows are those of the two known large teleseismic events that occurred on both sides of the Japan Trench in 2005 [e.g., *Uchida et al.*, 2006]. The tilt data also show presence of smaller but closer seismic events around NWP. The northward geomagnetic component (B_x) was drawn to illustrate overall geomagnetic activity of external origin during the seafloor observation period, which showed negligible correlation with the earthquakes. The impulses with a cross in Figure 3 (bottom) indicate the daily sum of K_p indices (ΣK_p). It also turned out geomagnetically very quiet at the time of the two tsunami events with K_p indices of 1 and 0 for 2006 and 2007, respectively.

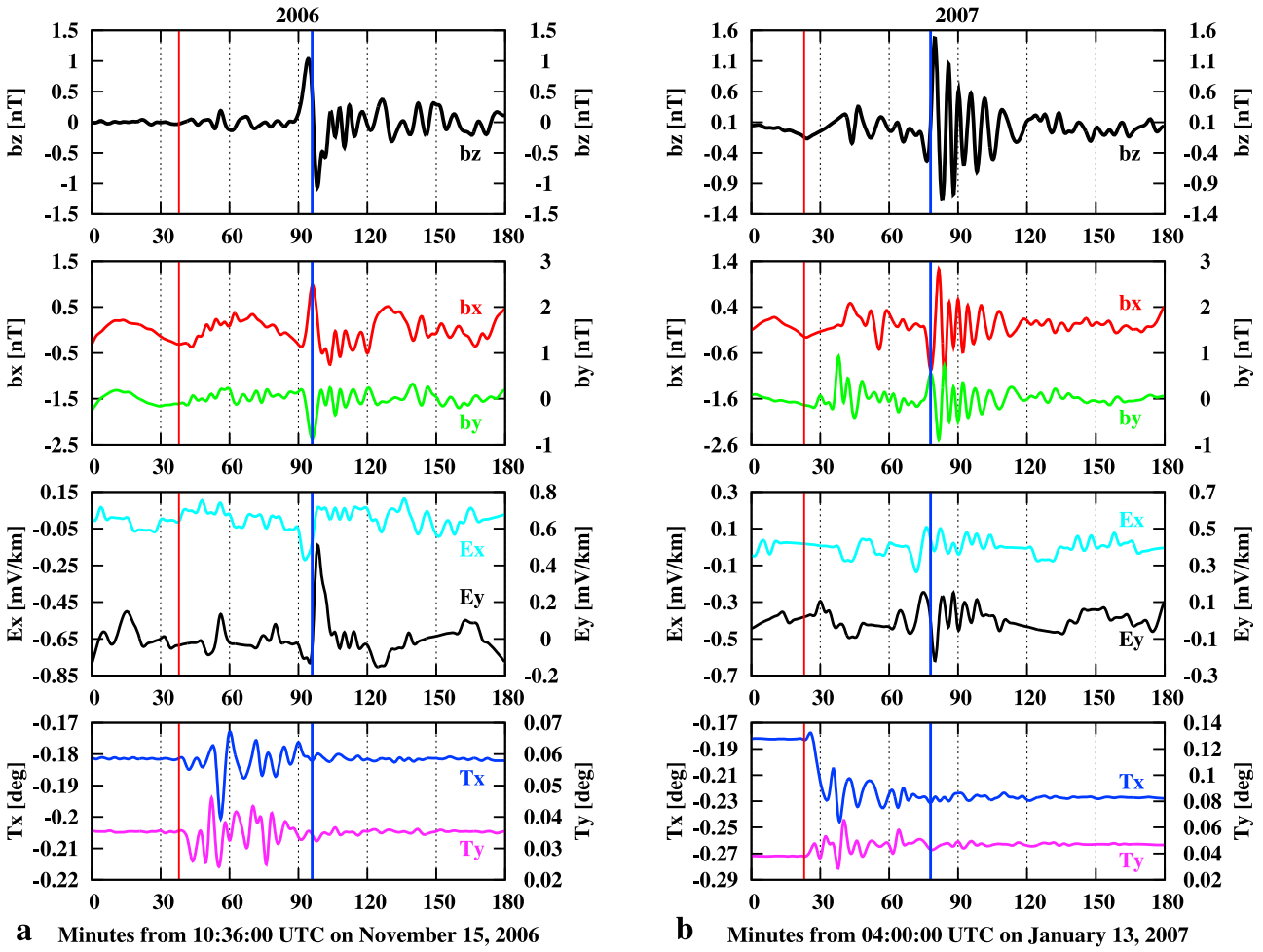

Figure 4. The 3 h plots of the observed time series at the time of the two Kuril earthquakes in (left) 2006 and (right) 2007. (top to bottom) The downward (b_z), northward (b_x), and eastward (b_y) geomagnetic components, horizontal geoelectric components (E_x and E_y), and horizontal tilts (T_x and T_y). The two vertical solid lines indicate the estimated time of arrival (ETA) of seismic and tsunami waves at NWP, respectively. Note that major variations of the seafloor EM components commenced only after those of tilts ceased. The tsunami ETAs coincide well with the peaks in the horizontal geomagnetic components.

where E_x, E_y, b_x and b_y are the northward electric, eastward electric, northward magnetic and eastward magnetic components of the tsunami-induced EM field, respectively [see *Sanford*, 1971]. μ and k are the magnetic permeability and the leakage constant [*Chave and Luther*, 1990] that is the ratio of the seafloor conductance to the ocean conductance. Equations (1) and (2) are valid when conductivity of the crust and the mantle is small enough. To evaluate their validity, let us assume the subseafloor conductivity, σ, be 10^{-2} S/m (somewhat too conductive crust and uppermost mantle) and the time scale of the tsunamis, T, be 10^3 s (very long tsunami duration). These values give us the upper limit of conductance $\left(= \sigma\delta = \frac{\sqrt{10\sigma T}}{2\pi} \times 10^3[\mathrm{S}]\right)$ for the crust and the mantle, where δ is the skin depth in the seafloor. The resultant subseafloor conductance is slightly less than 1600 S, only a 8.6% of the conductance of the ocean (~18000 S). This implies that contribution of the conductive crust and mantle is at least 1 order of magnitude smaller than that of the thick ocean above NWP. Equations (1) and (2), therefore, are applicable to our case at least to first approximation.

[7] The contribution of sediments can be argued negligible as follows: because the thickness of sedimentary layers beneath NWP is as thin as 375 m [*Shipboard Scientific Party*, 2001], the leakage constant k is as small as less than 2% (0.0168). This means that the motionally induced electric currents are mostly confined within the ocean in the present case. It is worth arguing what is expected for larger k. While the negligible k maximizes the contribution of the seafloor electric field to the particle motion estimates (see equations (1) and (2)), a k as large as unity makes the particle motions irrelevant to the seafloor electric field. This implies that the vector geomagnetic measurements become much more important for seafloor observatories in coastal regions with thick and conductive sediment accumulation than in open ocean observatories.

[8] According to *Key* [2003], noise levels of usual seafloor EM sensors are typically ~0.01 μV m$^{-1}\sqrt{Hz^{-1}}$ and ~0.1 nT$\sqrt{Hz^{-1}}$ at a period of 1000 s. Substitution of these values into equations (1) and (2) yields a threshold of $1.9 \times 10^{-8} F_z^{-1}$ m s^{-1} for seawater particle motion over a flat ocean

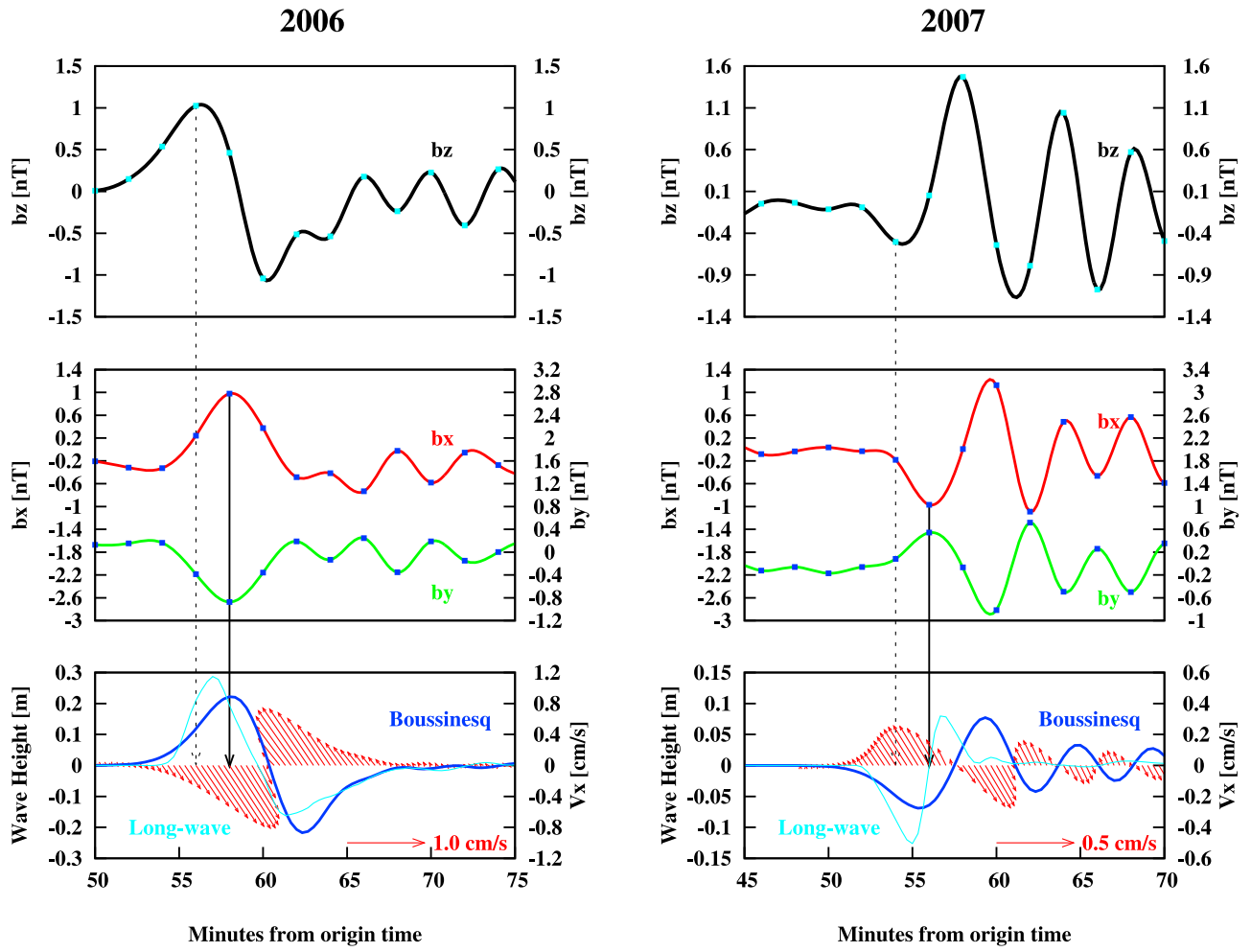

Figure 5. The 25 min plots covering each tsunami arrival of the (left) 2006 and (right) 2007 events. (top to bottom) Downward and two horizontal geomagnetic components and predicted tsunami height superimposed by particle velocity estimates. Square symbols indicate observed geomagnetic field values at NWP. The solid vertical arrows show coincidence of the peaks in the horizontal geomagnetic components with the maxima of tsunami height and particle velocity predicted by the Boussinesq approximation, while the dashed arrows show the peaks in the downward geomagnetic component always preceding the maximum tsunami heights.

of 4000 m deep. Even if the vertical geomagnetic component, F_z, is as small as 10000 nT (equivalent to a geomagnetic latitude of 10° for a purely dipolar geomagnetic main field), the tsunami-associated particle motion of seawater is detectable provided that it is larger than 2 mm s^{-1}. Hence, it can be concluded that geomagnetic observatories at the deep seafloor are capable of detecting tsunami-induced EM signals for tsunamigenic earthquakes larger than M8 in most of the oceanic areas other than equatorial regions.

3. Observed Signals

[9] In November 2006 and January 2007, a pair of tsunamigenic earthquakes occurred on both sides of the Kuril Trench [*Ammon et al.*, 2008], whose epicenters are 700–800 km away from our seafloor geomagnetic observatory coined NWP (Figure 2). As for details of each earthquake and NWP, refer to Table 1. The focal mechanism of the 2006 landward earthquake (M8.3, E1) was a shallow-dipping thrust type while that of the 2007 seaward earthquake (M8.1, E2) was of normal fault type [*Ammon et al.*, 2008]. Because of the opposite focal mechanisms, initial motions of the generated tsunamis were also opposite [*Fujii and Satake*, 2008] when observed at the same site. Since the tiltmeters of the seafloor geomagnetic observatory have noise levels as low as several arc seconds [*Toh et al.*, 2006], they responded to the arrival of seismic waves well (Figure 3). On the other hand, EM components showed significant changes only on and after the tsunami first arrival and were insensitive to the seismic waves (Figure 4). Although it is less clear in the 2007 event, the tsunami ETAs (Expected Time of Arrivals) coincide well with the unipolar peaks of the horizontal geomagnetic components, while the bipolar peaks of the downward geomagnetic component are prior to the unipolar peaks of the horizontal components (Figure 5) as mentioned in section 2. The time lead is, in principle (see Figure 1), equal to $T/4$, where T is the dominant period of the tsunami in concern.

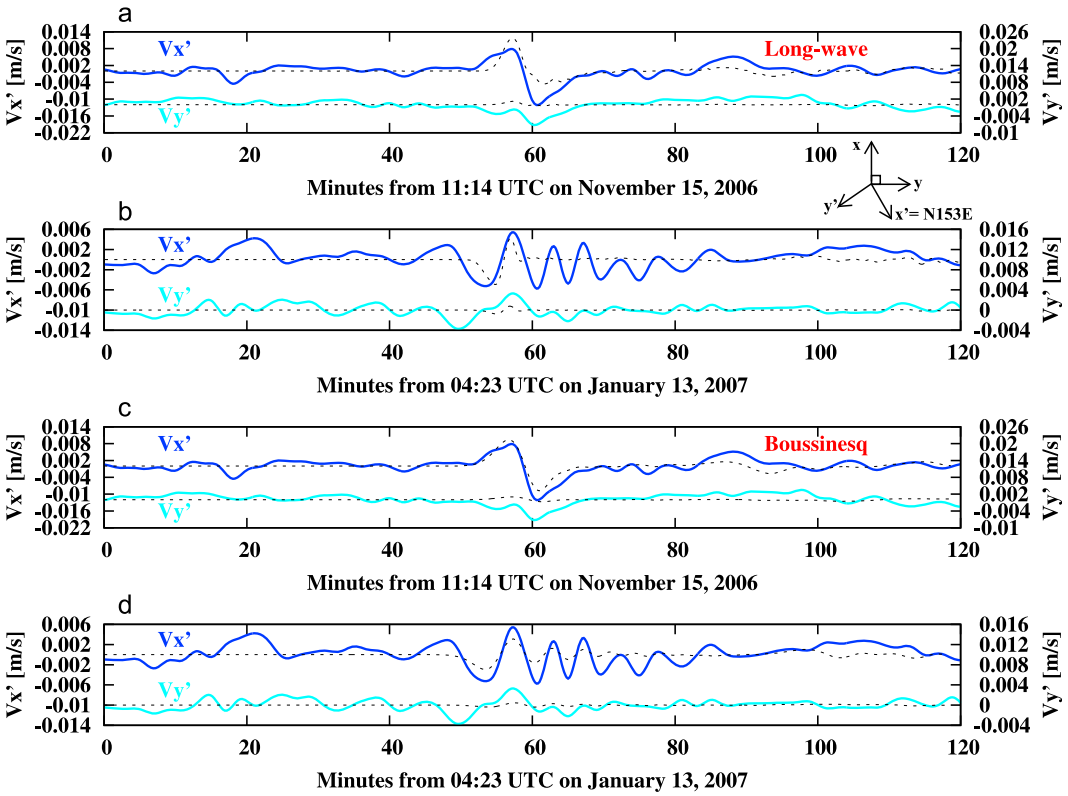

Figure 6. Comparison of electromagnetically (solid lines) and hydrodynamically (dashed lines) predicted particle motion by the (a and b) long-wave approximation and (c and d) the Boussinesq approximation for both tsunami events. The velocity components are in coordinates either parallel (x') or perpendicular (y') to the propagation direction of each tsunami. It is evident that the Boussinesq approximation reproduced the EM observation better than the long-wave approximation especially for the significant particle motion after the first arrival in 2007, suggesting a larger dispersion effect for the 2007 tsunami of shorter wavelength.

[10] Another unique feature of seafloor geomagnetic observatories as tsunami detectors is that they are intrinsically capable of vector measurements and hence estimation of tsunami front directions is possible even by single site observation. For example, the northward and eastward geomagnetic components changed +1.38 and −1.05 nT, respectively, at the first tsunami arrival in the 2006 event. This resulted in an estimate for the tsunami arrival direction of N323°E (=$\tan^{-1}(-1.05/1.38)$), which is in good agreement with the direction of the epicenter seen from NWP. The 2007 event also gave a similar directional estimate. Monitoring of the tsunami propagation direction is also possible in the postarrival phases of each tsunami event. The geomagnetic time series reported here is the first solid evidence of motionally induced magnetic field at the seafloor. It has been argued that the seafloor electric field is primarily sensitive to ocean currents [*Chave and Luther*, 1990] and observational efforts have been mostly confined to the seafloor electric field [*Luther et al.*, 1991; *Fujii and Chave*, 1999; *Nolasco et al.*, 2006]. However, provided that the motion of the seawater is sufficiently coherent as in the case of tsunamis, it can generate effective electric current circuits in the ocean to produce observable magnetic fields exceeding geomagnetic fluctuations of external origin. As for the motionally induced magnetic field observed at satellite altitudes, it has already been reported elsewhere [*Tyler et al.*, 2003].

4. Comparison of Detected EM Signals With Hydrodynamic Simulation

[11] In order to interpret the tsunami-induced EM signals, hydrodynamic simulation of the two tsunami events were conducted. The hydrodynamic calculations of the tsunamis in Figure 5 (bottom) and Animation S1 were conducted by finite difference methods for linear long-wave equation [*Fujii and Satake*, 2008] and linear Boussinesq equation [*Tanioka*, 2000].[1] The initial conditions were given by seafloor deformation calculated from heterogeneous slip distribution inferred from tsunami waveforms [*Fujii and Satake*, 2008]. The bathymetry used here was a 1 min mesh data compiled by General Bathymetric Chart of the Oceans (GEBCO, http://www.gebco.net/).

[12] Closer comparison of the vector geomagnetic field with hydrodynamic simulation results (Figure 5) shows that the peaks of the horizontal geomagnetic components are in agreement with the maxima of wave height and particle velocity at the tsunamis' first arrival, while those in the

[1] Auxiliary materials are available in the HTML. doi:10.1029/2010JB007873.

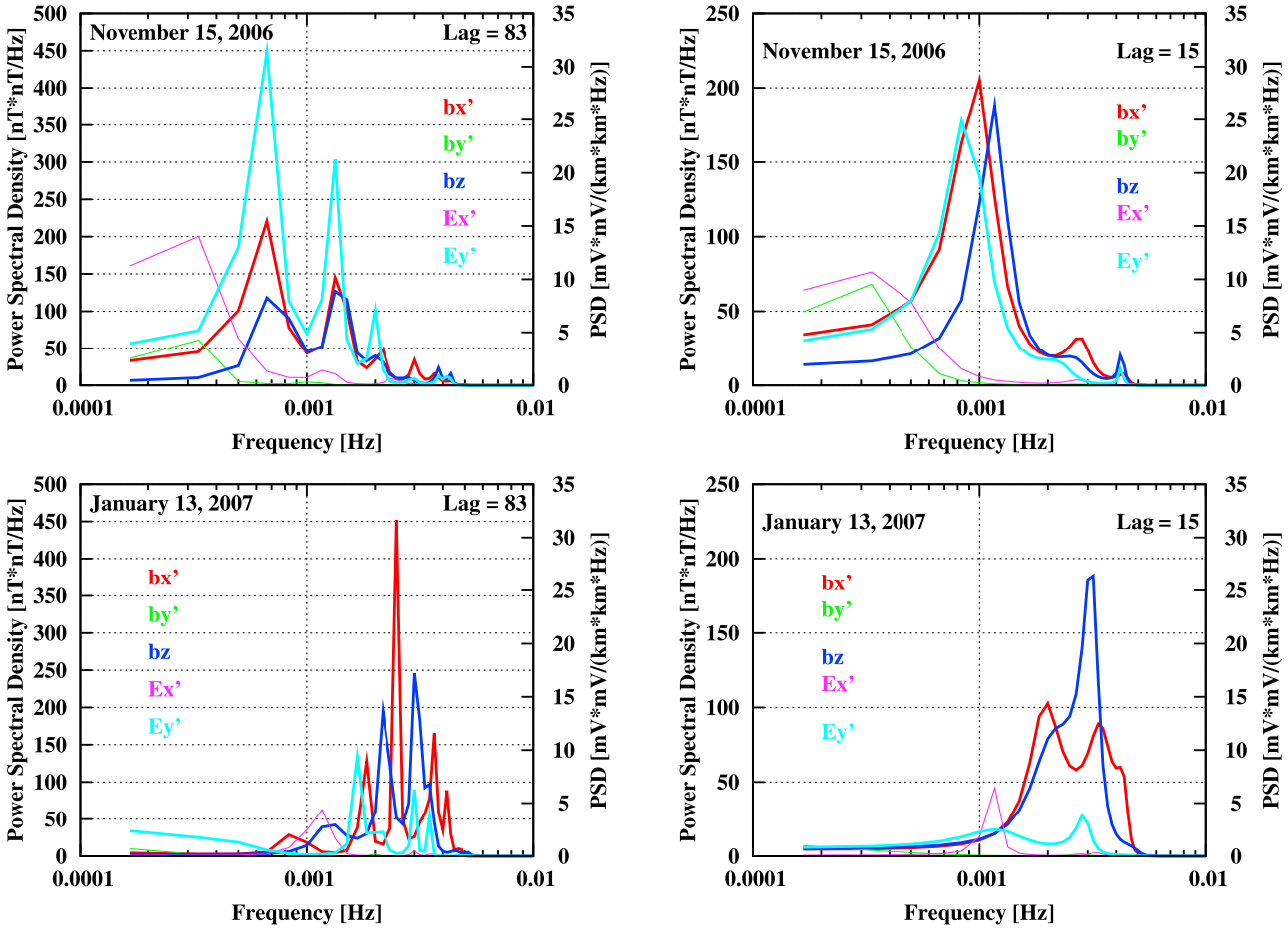

Figure 7. Power spectra of the tsunami-induced EM fields at the (top) 2006 and (bottom) 2007 events using the (left) largest possible and (right) optimized lags in the MEM analyses. It is evident that the 2006 tsunami was abundant in lower frequencies centered at 1 mHz, while the dominant frequency was approximately 3 mHz in 2007. Larger and broader spectral peaks also imply stronger tsunamis in 2006. Note that the incompatible EM components ($E_{x'}$ and $b_{y'}$, thin lines), parallel and perpendicular to the tsunami propagation direction, respectively, are small in magnitude and have significantly lower dominant frequencies. This implies that they may be irrelevant to the direct dynamo action by the tsunami particle motions.

downward geomagnetic component are seen before arrival in both events. Furthermore, the hydrodynamic simulation using Boussinesq approximation seems to yield dispersion effects that reproduced the large EM fluctuations seen in postarrival phases of the 2007 event (Figures 5 and 6 and Animation S1). We will confirm the dispersion effects by direct comparison of the observed and simulated particle velocities later in this section. Although the coarse sampling of the original time series (120 s) prevents further arguments on detailed time evolution of each tsunami event, response of the seafloor vector geomagnetic field to the initial motions of each tsunami is worth noting: signs of the magnetic field were reversed for a tsunami of opposite initial motion (Figure 5). This implies that it is electromagnetically distinguishable whether the tsunami height is positive or negative at the first arrival. This is important information in terms of disaster prevention because tsunamis with rise waves can be more dangerous than retreat waves when they hit the coast. In this context, seafloor geomagnetic observatories not only possess the same ability as deep ocean tsunami sensors (e.g., DART system) but also enable us to forecast tsunami arrivals by detecting precursors in the downward geomagnetic component.

[13] The detected EM signals can be converted into particle motion of the seawater associated with tsunamis using equations (1) and (2). Results of the conversion are shown in Figure 6 together with the hydrodynamically predicted tsunami particle motion. Note that the measuring frame has been rotated so as to make x' axis parallel to the magnetically determined direction of tsunami propagation at the first arrival. The electromagnetically estimated particle motion of each tsunami event is not only synchronized to the tsunamis' first arrival but also with the similar magnitude as the dynamically simulated velocity. For both events, the Boussinesq approximation fits better than the long-wave approximation, implying significant effects by finite wavelengths of the tsunamis. However, there appeared significant $V_{y'}$ component as well, which is incompatible with the electric current wall hypothesis depicted in Figure 1. Spectral analyses of the tsunami-induced EM variations were

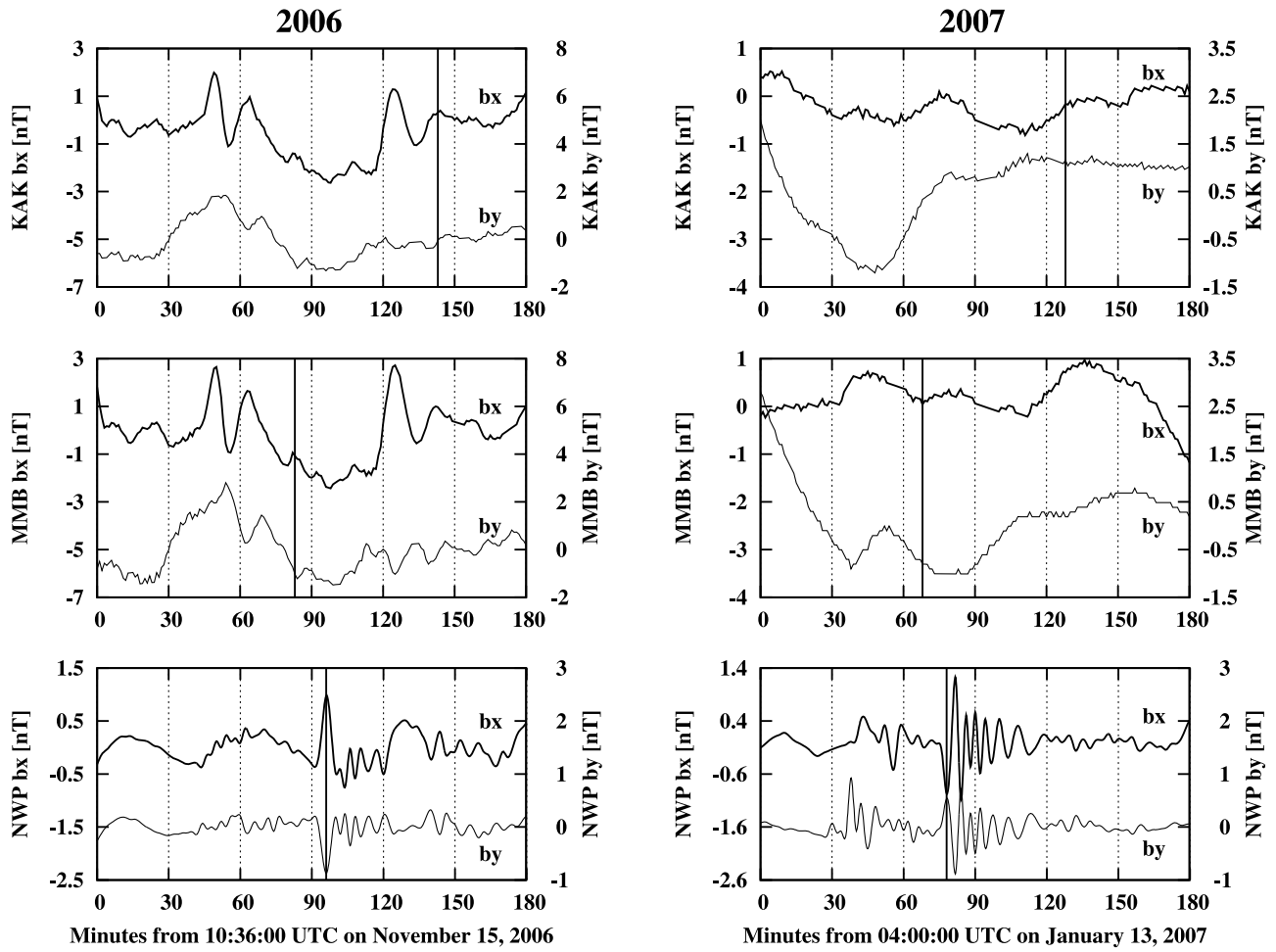

Figure 8. Comparison of horizontal geomagnetic time series observed (top and middle) on land and (bottom) at the seafloor. (left and right) Both tsunami events are drawn. Vertical solid lines are tsunami ETAs at each observatory. It is clear that there occurred no external disturbances at both tsunami ETAs of NWP. It is also evident that the land geomagnetic observatories recorded no significant changes at their tsunami ETAs.

conducted in order to estimate the wavelength of each tsunami as well as the origin of the incompatible velocity component.

[14] The dominant periods, *T*s, of the two tsunami events were determined using the maximum entropy method (MEM). The result (Figure 7) clearly shows that the 2006 event contained longer periods (and hence longer wavelengths) than the 2007 event irrespective to the number of lags used in the MEM analysis. Adopting *lag* = 15 that minimized the final prediction error [*Akaike*, 1969] of the MEM power spectra yielded dominant frequencies of 1 and 3 mHz for the 2006 and 2007 events, respectively. Those frequencies correspond to equivalent wavelengths of 234 km and 78 km, respectively. The shorter wavelength explains well why the 2007 tsunami showed more dispersive effects, i.e., presence of multiple waves after the first peak. It is noteworthy that power spectral density of EM components parallel ($E_{x'}$) and perpendicular ($b_{y'}$) to the tsunami fronts has smaller peaks at lower frequencies than other components ($E_{y'}$, $b_{x'}$ and b_z) that are compatible with the electric current wall hypothesis within the ocean. The incompatible EM components ($E_{x'}$ and $b_{y'}$), therefore, may have different origin other than the direct source current, $\boldsymbol{J}$.

[15] Another possibility is that coupling of the tsunami particle motion with the horizontal components of the geomagnetic main field (B_x and B_y) produces the EM components incompatible with the electric current wall hypothesis within the ocean. The coupling may particularly become significant for barotropic seawater flows like those of tsunamis with nearly identical horizontal motion all through the ocean layer. More specifically, the coupling of the horizontal geomagnetic components ends up with electromotive force in the vertical direction from the seafloor through the sea surface. However, the insulating Earth's atmosphere prevents the induced electric currents flowing out of the ocean. Surface charges are then accumulated so as to deflect the electric currents to form vertical loops in the ocean localized around tsunami wavefronts. The loops could be another cause of $V_{y'}$ component parallel to the tsunami wavefront in Figure 6. However, this qualitative argument

does not answer the question why the incompatible EM components have spectral peaks in lower frequencies.

5. Discussion and Conclusions

[16] It has been illustrated that the EM components at the seafloor in the northwest Pacific Ocean showed notable changes at the time of tsunami arrivals. On the other hand, it was also found that those signals were not recorded at land geomagnetic observatories (e.g., KAK and MMB), although it was geomagnetically very quiet at the time of the two tsunami events (K_p *index* [*Bartels*, 1949] = 1 and 0 in 2006 and 2007, respectively). It, therefore, is unlikely that the EM changes are due to external geomagnetic disturbances. Figure 8 illustrates the situation in more detail: (1) The horizontal geomagnetic components on land showed no significant changes at tsunami ETAs. NWP is the only site that responded to the tsunami arrivals. (2) Coherent variations at both land sites can be regarded as of external origin, which were negligible on the seafloor at the time of each tsunami ETA in 2007. The small variations at MMB around its tsunami ETA in 2006 turned out to be of external origin since we observe similar variations at KAK as well. These imply that seafloor geomagnetic observatories have much higher potential for detecting tsunami signals than land geomagnetic observatories.

[17] It has been shown that initial motions of tsunamis are electromagnetically distinguishable by examining signs of the horizontal tsunami-induced magnetic components (Figure 5). Although conventional tsunami sensors such as bottom pressure gauges are also able to discriminate positive and negative wave heights, seafloor EM sensors can provide the following three new information regarding tsunami properties: (1) Monitoring of the tsunami propagation direction by single site observation alone. (2) Enabling estimation of tsunami particle motions by the vector EM measurements. (3) Tsunami forecast by detecting the bipolar peak in the downward magnetic component that always precedes actual tsunami arrivals. It, therefore, is desirable that vector EM sensors will be integrated into the existing global tsunami warning systems for the sake of disaster mitigation.

[18] Comparison of the observed EM signals with the hydrodynamic simulation results in terms of tsunami particle motions has revealed that the linear Boussinesq approximation fits the EM observation better than the linear long-wave approximation especially for the 2007 tsunami of shorter wavelength (Figure 6). This is because the Boussinesq approximation can account for the larger dispersion effect on short-wavelength tsunamis much better than the long-wave approximation. However, the discrepancy between the EM and hydrodynamic estimates of particle motions is still significant. It may possibly be due to inaccuracy in converting the detected EM signals into the tsunami particle motion. The dominant frequencies of the two tsunami events range from 1 mHz to 3 mHz (Figure 7), which are large enough to cause self-induction effects in the tsunami-induced EM field. In other words, the tsunami-induced EM field can be modified by its own temporal variation, which requires us different conversion formulae other than equations (1) and (2) to appreciate the observed EM signals. It, therefore, is desirable to include the self-induction effect that is missing in *Sanford*'s [1971] theory of motional induction in the future.

[19] **Acknowledgments.** R/V *Kairei* and ROV *Kaiko7000II* of Japan Agency for Marine-Earth Science and Technology are greatly acknowledged for their skilful help at the time of sea experiments. H.T. expresses his sincere thanks to Earthquake Research Institute, University of Tokyo, for its continuous support throughout this study. Thorough reviews by K. Key and an anonymous referee were indispensable to improve our original manuscript. We are grateful to T. Higa at Faculty of Science, Kyoto University, for his careful processing of raw time series. This work is also supported by Grants in Aid for Scientific Research of MEXT, Japan (18204038 and 21654061).

References

Akaike, H. (1969), Fitting autoregressive models for prediction, *Ann. Inst. Stat. Math.*, *21*, 243–247, doi:10.1007/BF02532251.

Ammon, C. J., K. Kanamori, and T. Lay (2008), A great earthquake doublet and seismic stress transfer cycle in the central Kuril islands, *Nature*, *451*, 561–565, doi:10.1038/nature06521.

Bartels, J. (1949), The standardized index K_s, and the planetary index K_p, IATME Bull., 12(b), *97*, IUGG Publ. Office, Paris.

Bernard, E. N., and A. R. Robinson (2009), *Tsunamis, The Sea*, vol. 15, Harvard Univ. Press, Cambridge, Mass.

Bryan, F. (1987), Parameter sensitivity of primitive equation ocean general circulation models, *J. Phys. Oceanogr.*, *17*, 970–985, doi:10.1175/1520-0485(1987)017<0970:PSOPEO>2.0.CO;2.

Chave, A. D., and D. S. Luther (1990), Low-frequency, motionally induced electromagnetic fields in the ocean: 1.Theory, *J. Geophys. Res.*, *95*, 7185–7200, doi:10.1029/JC095iC05p07185.

Faraday, M. (1832), The Bakerian Lecture: Experimental researches in electricity–Second series, *Philos. Trans. R. Soc. London*, *122*, 163–194, doi:10.1098/rstl.1832.0007.

Fujii, I., and A. D. Chave (1999), Motional induction effect on the planetary scale geoelectric potential in the eastern North Pacific, *J. Geophys. Res.*, *104*, 1343–1359, doi:10.1029/1998JC900041.

Fujii, Y., and K. Satake (2008), Tsunami sources of the November 2006 and January 2007 great Kuril earthquakes, *Bull. Seismol. Soc. Am.*, *98*, 1559–1571, doi:10.1785/0120070221.

Key, K. (2003), Application of broadband marine magnetotelluric exploration to a 3D salt structure and a fast-spreading ridge, Ph.D. thesis, Dep. of Earth Sci., Univ. of Calif., San Diego, La Jolla.

Larsen, J. C., and T. B. Sanford (1985), Florida current volume transports from voltage measurements, *Science*, *227*, 302–304, doi:10.1126/science.227.4684.302.

Lay, T., et al. (2005), The great Sumatra-Andaman earthquake of December 26, 2004, *Science*, *308*, 1127–1133, doi:10.1126/science.1112250.

Longuet-Higgins, M. S. (1949), The electric and magnetic effects of tidal streams, *Geophys. J. Int.*, *5*, suppl., 285–307.

Luther, D. S., J. H. Filloux, and A. D. Chave (1991), Low-frequency, motionally induced electromagnetic fields in the ocean: 2. Electric field and Eulerian current comparison, *J. Geophys. Res.*, *96*, 12,797–12,814, doi:10.1029/91JC00884.

Nolasco, R., A. Soares, J. M. Dias, F. A. M. Santos, N. A. Palshin, P. Represas, and N. Vaz (2006), Motional induction voltage measurements in estuarine environments: The Ria de Aveiro Lagoon (Portugal), *Geophys. J. Int.*, *166*, 126–134, doi:10.1111/j.1365-246X.2006.02936.x.

Sanford, T. B. (1971), Motionally induced electric and magnetic fields in the sea, *J. Geophys. Res.*, *76*, 3476–3492, doi:10.1029/JC076i015p03476.

Satake, K., S. Sakai, T. Kanawaza, Y. Fujii, T. Saito, and T. Ozaki (2010), The February 2010 Chilean tsunami recorded on bottom pressure gauges, paper presented at Japan Geoscience Union Meeting, Abstract MIS050–P05.

Segawa, J., and H. Toh (1992), Detecting fluid circulation by electric field variations at the Nankai Trough, *Earth Planet. Sci. Lett.*, *109*, 469–476, doi:10.1016/0012-821X(92)90107-7.

Shipboard Scientific Party (2001) Site 1179, *Proc. Ocean Drill. Program, Initial Rep.*, *191*, 1–159, doi:10.2973/odp.proc.ir.191.104.2001.

Tanioka, Y. (2000), Numerical simulation of far-field tsunamis using the linear Boussinesq equation–The 1998 Papua New Guinea Tsunami, *Pap. Meteorol. Geophys.*, *51*, 17–25, doi:10.2467/mripapers.51.17.

Titov, V., A. B. Rabinovich, H. O. Mofjeld, R. E. Thomson, and F. I. González (2005), The global reach of the 26 December 2004 Sumatra Tsunami, *Science*, *309*, 2045–2048, doi:10.1126/science.1114576.

Toh, H., Y. Hamano, M. Ichiki and H. Utada (2004), Geomagnetic observatory operates at the seafloor in the northwest Pacific Ocean, *Eos Trans. AGU*, *85*(45), doi:10.1029/2004EO450003.

Toh, H., Y. Hamano, and M. Ichiki (2006), Long-term seafloor geomagnetic station in the northwest Pacific: A possible candidate for a seafloor geomagnetic observatory, *Earth Planets Space*, *58*, 697–705.

Toh, H., Y. Hamano, and T. Goto (2009), Tsunami-induced electromagnetic fields at the seafloor caused by earthquakes on both sides of the Kuril trench, *Eos Trans. AGU*, *90*(52), Fall Meet. Suppl., Abstract GP43C–03.

Tyler, R., S. Maus, and H. Lühr (2003), Satellite observations of magnetic fields due to ocean tidal flow, *Science*, *299*, 239–241, doi:10.1126/science.1078074.

Uchida, N., T. Matsuzawa, S. Hirahara, and A. Hasegawa (2006), Small repeating earthquakes and interplate creep around the 2005 Miyagi-oki earthquake (M = 7.2), *Earth Planets Space*, *58*, 1577–1580.

Y. Fujii, International Institute of Seismology and Earthquake Engineering, Building Research Institute, Tsukuba, Ibaraki 3050802, Japan.

T. Goto, Graduate School of Engineering, Kyoto University, Katsura, Nishikyo-ku, Kyoto 6158540, Japan.

Y. Hamano, Institute for Research on Earth Evolution, Japan Agency for Marine-Earth Science and Technology, Yokosuka, Kanagawa 2370061, Japan.

K. Satake, Earthquake Research Institute, University of Tokyo, Yayoi, Bunkyo-ku, Tokyo 1130032, Japan.

H. Toh, Data Analysis Center for Geomagnetism and Space Magnetism, Kyoto University, Kitashirakawa'oiwake-cho, Sakyo-ku, Kyoto 6068502, Japan.